

Non-Abelian fractionalization in topological minibands

Aidan P. Reddy,* Nisarga Paul,* Ahmed Abouelkomsan, and Liang Fu

Department of Physics, Massachusetts Institute of Technology, Cambridge, Massachusetts 02139, USA

(Dated: March 21, 2024)

Motivated by the recent discovery of fractional quantum anomalous Hall states in moiré systems, we consider the possibility of realizing non-Abelian phases in topological minibands. We study a family of moiré systems, skyrmion Chern band (SCB) models, which can be realized in two-dimensional semiconductor/magnetic skyrmion heterostructures and also capture the essence of twisted transition metal dichalcogenide (TMD) homobilayers. We show using many-body exact diagonalization that, in spite of strong Berry curvature variations in momentum space, the non-Abelian Moore-Read state can be realized at half filling of the second miniband. These results demonstrate the feasibility of non-Abelian fractionalization in moiré systems without Landau levels and shed light on the desirable conditions for their realization. In particular, we highlight the prospect of realizing the Moore-Read state at filling factor $\nu = 3/2$ in twisted semiconductor bilayers.

The fractional quantum Hall (FQH) effect has traditionally been limited to the context of two-dimensional electron systems in a strong magnetic field. Remarkably, recent experiments have observed a sequence of FQH states in twisted bilayer semiconductor $t\text{MoTe}_2$ [1–4] and rhombohedral pentalayer graphene/hBN [5] at *zero* field. In twisted bilayer semiconductors, the existence of such fractional quantum anomalous Hall (FQAH) states was theoretically predicted [6–8] as a consequence of Coulomb interactions in partially filled topological moiré bands [9] and spontaneous time-reversal symmetry breaking. Fractional and integer QAH states have also been proposed in other moiré material platforms, including twisted bilayer graphene [10–13], periodically strained graphene [14, 15] and narrow gap semiconductors subject to an electrostatic superlattice potential [16, 17]. These theoretical advances and experimental breakthroughs introduce a new frontier of strongly correlated topological quantum matter and offer the potential to achieve high-temperature topological protection.

To date, much work on the FQAH effect has focused on filling factors $\nu < 1$. Here, theoretical understanding is largely guided by the resemblance between the $|C| = 1$ band (C is the band Chern number) and the lowest Landau level (LLL). At fractional filling of a Chern band, Coulomb interaction can drive the system into fractional Chern insulator (FCI) states—the lattice analog of FQH states [18–22]. A natural question is how far this guiding principle can be pushed to higher fillings.

While the LLL typically hosts Abelian topological orders at fractional fillings, the first excited Landau level (1LL) is predicted to host even richer *non-Abelian* topological orders [23], e.g. the phase of the Moore-Read Pfaffian/ anti-Pfaffian state [24–26] or the Read-Rezayi state [27]. These phases support fractional quasiparticles obeying non-Abelian exchange statistics [28–31] and could provide a platform for fault-tolerant quantum computation [32–34]. Theoretical studies have also explored non-Abelian phases of fermions and bosons in lattice models [35–37] as well as quantum spin systems [38, 39]. The

advent of FQAH materials raises the exciting prospect of realizing non-Abelian fractionalization without a magnetic field and at elevated temperatures.

As a starting point, we note that theory predicts that the second moiré band in twisted transition metal dichalcogenide ($t\text{TMD}$) homobilayers is flat, well isolated, and has the same sign Chern number as the first moiré band over a wide range of twist angles [6, 40]. In these respects, it resembles the 1LL. As such, we consider whether non-Abelian FQAH states at higher filling factors may be formed in the second band in $t\text{TMDs}$. In particular, we study a family of continuum models, *skyrmion Chern band* models, which captures in a minimal setting the essential features of topological minibands in twisted TMD bilayers (such as $t\text{MoTe}_2$ and $t\text{WSe}_2$) as well as other material platforms. Within this family of models, including an adiabatic approximation to a continuum model for $t\text{MoTe}_2$ [41], we establish using many-body exact diagonalization that the analog of the non-Abelian state in the half-filled $n = 1$ LL can be realized in the second topological miniband. Our study provides a realistic material proposal for realizing non-Abelian phases in topological minibands and sheds light on the desirable conditions for their realization.

The following simple Hamiltonian defines our family of skyrmion Chern band (SCB) models in two dimensions:

$$H = \frac{p^2}{2m} + J\boldsymbol{\sigma} \cdot \mathbf{S}(\mathbf{r}). \quad (1)$$

Here, $\boldsymbol{\sigma}$ is the spin (or pseudospin) degree of freedom and $\mathbf{S}(\mathbf{r}) = \mathbf{S}(\mathbf{r} + \mathbf{a}_{1,2})$ is a periodic spin texture, with J the exchange energy. We assume $\mathbf{S}(\mathbf{r})$ is a noncoplanar (chiral) texture that defines a mapping of the real-space unit cell (a torus) to the Bloch sphere with a nonzero winding number, such as a *skyrmion* texture. It is well known that chiral textures give rise to an emergent real-space magnetic field $B^e(\mathbf{r}) = \frac{\hbar}{2e} \hat{\mathbf{S}} \cdot (\partial_x \hat{\mathbf{S}} \times \partial_y \hat{\mathbf{S}})$, with an integer number of flux quanta per unit cell ($\hat{\mathbf{S}} = \mathbf{S}/S$). The resulting “topological Hall effect” has been widely studied

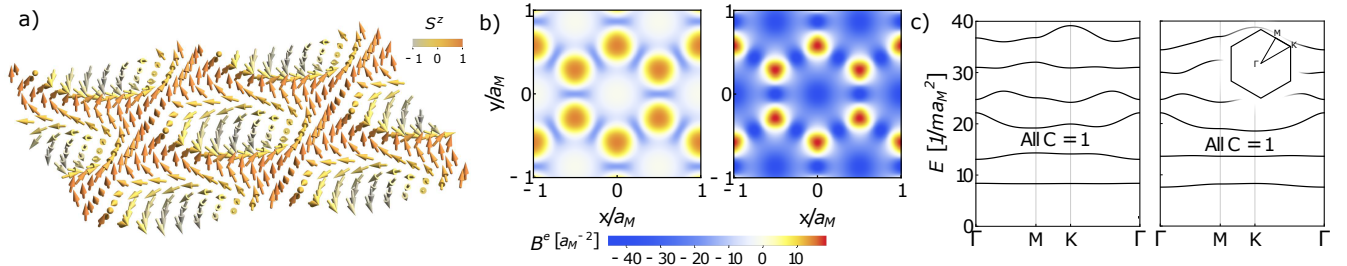


FIG. 1. **Skyrmion Chern band (SCB) models.** Electrons strongly coupled to a skyrmion-like spin or pseudospin texture may exhibit flat topological minibands. (a) An example texture ($\alpha = 1, N_0 = 0.11$). (b) Emergent magnetic field B^e , or scalar chirality, associated with skyrmion textures (from part (a), on left; with $\alpha = 1.5, N_0 = 0.4$, on right). (b) Respective electronic bandstructures, which exhibit flat first or second topological minibands. Energy measured from $-J$ at large J .

in magnetic metals [42, 43]. On the other hand, skyrmion textures have been less studied in low-density semiconductors. Here, the topological Hall effect manifests as a quantized anomalous Hall effect due to the formation of Chern bands [44]. In a recent work [45], we showed that remarkably, these Chern bands can become *flat* at a magic value of the magnetization $\bar{m} = \langle S^z \rangle$. SCB models can be potentially realized in a two-dimensional (2D) semiconductor proximity-coupled to a magnetic insulator. In Ref. [45] the heterostructure $\text{MoS}_2/\text{CrBr}_3$ is proposed which has the following advantages: a large exchange energy J , and the likelihood of a skyrmion crystal (SkX) even at zero field in chromium trihalide bilayers [46–48].

As we now describe, the combination of large J ($J \gg \hbar^2/m a_M^2$, where a_M is the moiré period and m is the effective mass of charge carriers) and an SkX allows for flat Chern bands. The large- J or “adiabatic” limit, which is generally achievable [45], enforces local alignment of the electron spin to $\mathbf{S}(\mathbf{r})$, which in turn induces a Berry phase. This is made clear by a position-dependent SU(2) unitary transformation $\mathbf{U}(\mathbf{r})$ which rotates the spin texture $\mathbf{S}(\mathbf{r})$ into $S(\mathbf{r})\hat{z}$ and introduces a gauge field $\mathbf{A}_i = \frac{i\hbar}{e}\mathbf{U}^\dagger \partial_i \mathbf{U}$. For large J , we may project into the low-energy manifold of locally spin (anti)-aligned electrons and obtain the effective Hamiltonian [45, 49]

$$H_{\text{eff}} = \frac{(\mathbf{p} - e\mathbf{A}(\mathbf{r}))^2}{2m} + \frac{\hbar^2}{8m}(\partial_i \hat{\mathbf{S}})^2 - JS(\mathbf{r}) \quad (2)$$

(summing $i = x, y$), where now $\mathbf{A}(\mathbf{r})$ is the $\downarrow\downarrow$ component of the SU(2) gauge field and the second term originates from its off-diagonal elements. We refer to \mathbf{A} as the emergent gauge field, with $\text{curl } B^e(\mathbf{r}) = \frac{\hbar}{2e}\hat{\mathbf{S}} \cdot (\partial_x \hat{\mathbf{S}} \times \partial_y \hat{\mathbf{S}})$, which is generally nonuniform. A skyrmion texture is one with a single flux quantum of emergent magnetic field B^e per unit cell, and is the simplest topologically nontrivial periodic spin texture. Eq. (2) establishes a parallel with ordinary Landau levels.

Indeed, TMD homobilayers are approximate SCB models with the role of σ played by the layer degree of freedom and their Chern bands can be understood

in a similar fashion [9, 41]. In this case, the layer-pseudospin skyrmion texture corresponds to interlayer tunnelings and intralayer potentials within the K and K' valleys that vary spatially according to local interlayer stacking [9]. Over a wide range of fillings, charge carriers are driven into one valley by Coulomb interactions, spontaneously breaking time-reversal symmetry [8, 40, 50]. The lowest band can be made flat by tuning twist angle [6, 41], which creates favorable conditions for FQAH states [7, 8, 40, 51–53].

We now proceed to study the model defined by Eq. (2), further assuming $S(\mathbf{r})$ is constant (a natural assumption for 2D magnets) to drop the final term. For the skyrmion texture, we adopt a simple ansatz built out of three harmonics. In particular, we take $\mathbf{S}(\mathbf{r}) = \mathbf{N}(\mathbf{r})/N(\mathbf{r})$ with

$$\mathbf{N}(\mathbf{r}) = \frac{1}{\sqrt{2}} \sum_{j=1}^6 e^{i\mathbf{q}_j \cdot \mathbf{r}} \hat{\mathbf{e}}_j + N_0 \hat{z} \quad (3)$$

where $\mathbf{q}_j = \frac{4\pi}{\sqrt{3}a_M}(\cos \theta_j, \sin \theta_j)$ and $\hat{\mathbf{e}}_j = (i\alpha \sin \theta_j, -i\alpha \cos \theta_j, -1)/\sqrt{2}$ and the angles satisfy $\theta_2 = \theta_1 + 2\pi/3, \theta_3 = \theta_1 + 4\pi/3$, and $\theta_{j+3} = \theta_j + \pi$. This texture can be thought of as a normalized sum of three spin spirals forming a triangular SkX, as plotted in Fig. 1a. It is widely adopted in studies of chiral magnets and magnetic skyrmion crystals, and qualitatively reproduces the real-space images of skyrmion crystals [54–58]. The parameter α controls coplanarity, while N_0 controls the out-of-plane magnetization $\bar{m} = \langle S^z \rangle$ (which monotonically increases with N_0). We will refer to the Hamiltonian defined with the skyrmion texture 3 as the SkX model.

In Fig. 1b we plot the emergent magnetic field for two examples textures, along with their associated large- J bandstructures in Fig. 1c. Even when $B^e(\mathbf{r})$ is highly nonuniform and changes sign within the unit cell, we observe that the topological minibands can be made quite flat. This is corroborated in Fig. 2, where we plot bandwidths and Berry curvature standard deviations for the lowest two bands across a range of parameters α and \bar{m} . Both quantities have a “magic line” in this param-

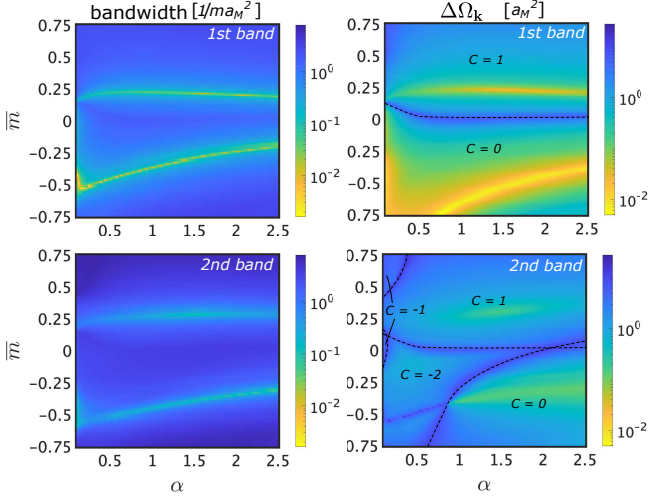


FIG. 2. **Band properties.** (Left) Bandwidths and (right) Berry curvature standard deviations of the two lowest bands in the SCB model as a function of coplanarity α and average S^z -magnetization \bar{m} . Bands exhibit minima in similar regions.

ter space, meaning they can be made relatively small by tuning a single parameter. Remarkably, we show in the following that a non-Abelian state can be stabilized even when the Berry curvature fluctuates wildly.

We now study many-body physics at filling $\nu = \frac{3}{2}$ (that is, half-filling of the second miniband) via numerical diagonalization. From here on, to enable direct comparison with Landau levels, we work with the effective Hamiltonian, Eq. 2. The natural energy unit that sets the average miniband gap is the effective cyclotron energy, $\hbar\omega_c = 2\pi\hbar^2/(mA_{uc})$. Although the full and effective SCB Hamiltonians, Eqs. 1 and 2, are defined on different Hilbert spaces, all low-energy physical quantities associated with the two Hamiltonians are identical in the limit $J/(\hbar\omega_c) \rightarrow \infty$.

To make the many-body calculation tractable, we restrict our variational Hilbert space to that in which N_{uc} electrons fill the lowest band and $N_e - N_{uc}$ electrons remain in the second miniband where N_e is the number of electrons. The filled lowest band produces a Hartree-Fock self-energy $\Sigma(\mathbf{k})$ for particles in the second band that is accounted for with a renormalized single-particle energy dispersion, $\tilde{\varepsilon}(\mathbf{k}) = \varepsilon(\mathbf{k}) + \Sigma(\mathbf{k})$. Here, $\varepsilon(\mathbf{k})$ is the non-interacting dispersion of the second miniband. Explicitly, we numerically diagonalize the effective projected Hamiltonian

$$\bar{H} = \sum_{\mathbf{k} \in BZ} \tilde{\varepsilon}(\mathbf{k}) n(\mathbf{k}) + \frac{1}{2A} \sum_{\mathbf{q}} v(\mathbf{q}) \bar{\rho}(-\mathbf{q}) \bar{\rho}(\mathbf{q}) \quad (4)$$

where $n(\mathbf{k}) = c_{2,\mathbf{k}}^\dagger c_{2,\mathbf{k}}$, $\bar{\rho}(\mathbf{q}) = P_2 \sum_i e^{-i\mathbf{q} \cdot \mathbf{r}_i} P_2$, and $v(\mathbf{q}) = \frac{2\pi e^2}{|\mathbf{q}|}$ is the Fourier transform of the Coulomb potential. P_2 is a projector onto the Fock space of the sec-

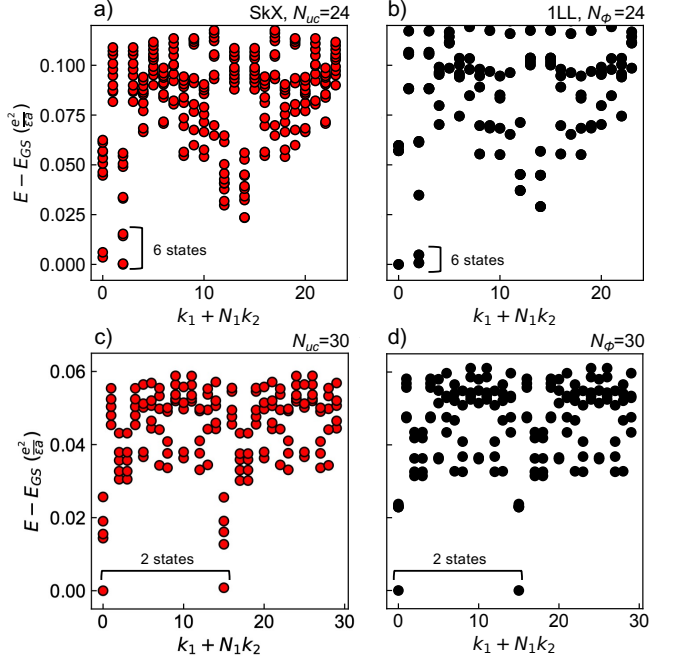


FIG. 3. **Exact diagonalization evidence.** (a) Low-energy many-body spectrum of the effective projected Hamiltonian Eq. 4 at half-filling of the second miniband computed via numerical diagonalization on a torus containing 24 unit cells, and (b) corresponding calculation of the 1LL. (c,d) Analogous data from a system containing 30 unit cells/flux quanta. The 10 (a,b) and 5 (c,d) lowest energy levels in each quasi-momentum sector are shown. $\alpha = 1$, $N_0 = 0.28$ (equivalently, $\bar{m} = 0.271$), and we set $\sqrt{\frac{4\pi}{3}} \frac{e^2}{\epsilon a} = \hbar\omega_c$.

ond miniband and $c_{2,\mathbf{k}}^\dagger$ creates a (magnetic) Bloch state in the second miniband.

In Fig. 3, we show many-body spectra obtained by diagonalizing \bar{H} on two finite-size toruses. For $N_{uc} = 24$, the number of electrons occupying the second miniband is even (12), while for $N_{uc} = 30$, it is odd (15). In the two cases, we observe sixfold and two-fold ground state quasi-degeneracies. (The finite-size splitting among these quasi-degenerate states decreases with increasing interaction strength.) These are precisely the degeneracies expected for a Moore-Read state on the torus due to an even-odd effect [25, 59], providing substantial evidence for a non-Abelian order. Moreover, the quasi-degenerate ground states have the same center-of-mass quasimomenta as the Coulomb ground state of the 1LL on the same finite system, matching those expected of the Moore-Read wavefunction [60, 61].

Besides the ground state degeneracy, mounting numerical evidence suggests that the Coulomb ground state of half-filled 1LL is a non-Abelian Moore-Read state [62]. However, its precise topological order is not fully determined [63]. In part, this is because the Moore-Read Pfaffian wavefunction breaks particle-hole symmetry [64–

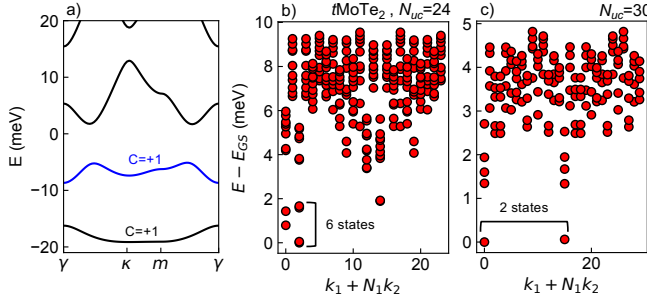


FIG. 4. **Adiabatic model for $t\text{MoTe}_2$.** (a) Minibands of the adiabatic model for $t\text{MoTe}_2$ at $\theta = 2.5^\circ$ with parameters from Ref. [40]. Exact diagonalization spectra on 24 (b) and 30 (c) unit cell clusters, showing the expected topological ground state quasi-degeneracies of the Moore-Read state (cf. Fig. 3) ($\theta = 2.5^\circ$, $\epsilon = 5$).

66]. Further, the particle-hole conjugate of the Pfaffian – the anti-Pfaffian – has distinct topological order reflected by, for instance, its distinct quantized thermal Hall conductance [63, 67, 68]. Neither candidate state can be an exact eigenstate of a LL-projected Hamiltonian with a two-body interaction on a torus, which has an exact particle-hole symmetry, at finite size.

In contrast to an ordinary Landau level, our system’s band-projected Hamiltonian lacks particle-hole symmetry. Therefore, its ground state should be non-particle-hole-symmetric. The ground state degeneracy shown above is compatible with either the Pfaffian or the anti-Pfaffian state. More studies are needed to determine the exact topological order.

Having established a Moore-Read state in the SkX model, we now turn to twisted TMDs. The layer pseudospin texture in $t\text{TMDs}$ differs from the spin texture of the SkX model: it has different spatial symmetry and contains two merons (half skyrmions) rather than a single skyrmion per unit cell. Additionally, its emergent magnetic field comprises sharp peaks forming a kagome lattice and its pseudospin field strength $S(\mathbf{r})$ is non-uniform [41].

Despite these differences, we find essentially the same evidence for a Moore-Read state at $\nu = \frac{3}{2}$ in $t\text{MoTe}_2$ as in the SkX model above. Our ED calculation (assuming full spin/valley polarization) for $t\text{MoTe}_2$ under the adiabatic approximation [41] is shown in Fig. 4(b-c). Our results show that a broad class of SCB models can host non-Abelian topological orders and indicate the possibility of their realization in twisted TMD homobilayers.

We now address the question of why SCB models host incompressible states in the second miniband resembling that of the 1LL. A natural way to quantify the similarity between the i^{th} SCB miniband and the corresponding LL

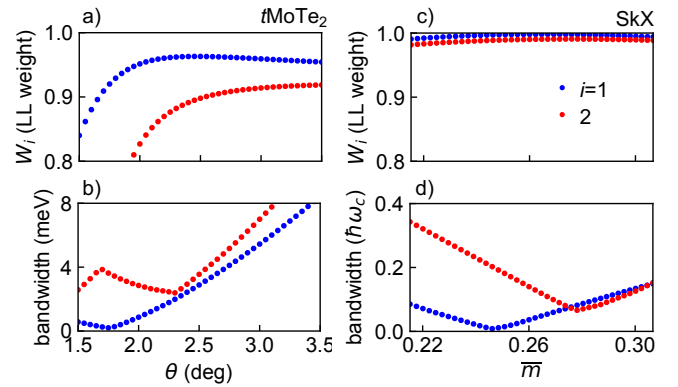


FIG. 5. **LL weight and bandwidth.** (a) LL weight W_i (Eq. 5) and (b) bandwidth of the lowest two minibands of the adiabatic model for $t\text{MoTe}_2$ with parameters from Ref. [40]. (c,d) Analogous quantities for the SkX model at fixed $\alpha = 1$ as a function of average spin texture magnetization \bar{m} .

is through the “LL weight”,

$$W_i = \frac{1}{N_{uc}} \sum_{\mathbf{k}} \left| \langle \psi^{(i)}(\mathbf{k}) | \psi_{\text{LL}}^{(i-1)}(\mathbf{k}) \rangle \right|^2. \quad (5)$$

In spite of the magnetic field and scalar potential fluctuations present in the effective Hamiltonian Eq. 2, its LL weights turn out quite high. In Fig. 5(a,b), we show the LL weights of the lowest two minibands in the adiabatic model for $t\text{MoTe}_2$. Over a broad range of twist angles the LL weights of the first and second minibands remain high, $> 90\%$. While the LL weights vary smoothly with interlayer twist θ , the bandwidths show cusp minima at “magic” values of θ [6, 41]. At small twist angles, the low-energy wavefunctions tend to localize in real space about maxima in $S(\mathbf{r})$ and form bands with low LL weights. At large twist angles, LL weights become larger but the adiabatic approximation becomes less accurate because kinetic energy increases relative to J . The lowest two bands of the SkX model exhibit even higher LL weights than the $t\text{TMD}$ adiabatic model, $> 99\%$ (Fig. 5(c,d)).

Remarkably, we find that even when the LL weight is very close to 1, Berry curvature can vary strongly throughout the Brillouin zone. For instance, given the SkX model parameters of Fig. 3, the LL weight of the second band is 0.989, yet the Berry curvature, in units such that its average is unity, ranges from 0.16 to 1.53 with a standard deviation of 0.38. The Berry curvature in the adiabatic $t\text{MoTe}_2$ model fluctuates even more strongly, varying from -3.4 to $+4.3$ with a standard deviation of 3. Notably, the quantum weight $K = \frac{1}{2\pi} \int d^2\mathbf{k} \text{Tr}(g(\mathbf{k}))$, where $g(\mathbf{k})$ the Fubini-Study metric [69, 70], is ~ 3.02 for the SkX model and ~ 3.23 for the adiabatic $t\text{MoTe}_2$ model – both close to the value of the 1LL (3 and $2n+1$ for the $n\text{LL}$ [71]).

In conclusion, we have shown that a family of skyrmion Chern band (SCB) models with two-body Coulomb inter-

actions host Moore-Read fractional quantum anomalous Hall states. SCB models are naturally realized in 2D semiconductors proximity-coupled to 2D magnets [45], and approximate the TMD systems in which Abelian FQAH states have been observed [1–4, 9]. At filling $\nu = \frac{3}{2}$, our many-body exact diagonalization exhibits the topological degeneracy expected of the Moore-Read state, including the even-odd effect [59], in close parallel with the 1LL [23]. While the extensive phase diagram of the SCB models is a fascinating problem, we opted to simply demonstrate the existence of a non-Abelian phase.

The realization of non-Abelian topological order in any setting carries with it significant challenges and equally significant reward. In moiré systems, these challenges could be mitigated by the exceptional degree of tunability. Moreover, our work shows that the necessary conditions are far less stringent than might have been thought, and band properties can deviate significantly from those of the 1LL. For instance, Berry curvature can be *far* from uniform.

Finally, we note that there is evidence for nontrivial topology and ferromagnetism in the second miniband of *t*TMDs. In particular, *double* quantum spin Hall states at $\nu = 4$ in *t*MoTe₂ and *t*WSe₂ [6, 72, 73], enabled by time-reversal symmetry and robust S_z /valley conservation, indicate that the first two moiré bands of a given spin/valley have Chern numbers of the same sign [9, 40]. Further, small-angle *t*MoTe₂ devices show large anomalous Hall resistance in the range $1 < \nu < 2$ [72], indicating spontaneous spin polarization. Full spin polarization may enable a non-Abelian FCI state at filling factor $\nu = \frac{3}{2}$, as in monolayer WSe₂ under a large magnetic field [74, 75], rather than at $\nu = \frac{5}{2}$ as in GaAs 2DEGs. These observations are promising for the prospect of an FCI state in *t*TMDs with non-Abelian topological order at filling $\nu = \frac{3}{2}$.

Acknowledgements— We thank Yang Zhang for collaboration on Ref.[45]. We thank Kin Fai Mak, Jie Shan, Kaifei Kang and Emil Bergholtz for stimulating discussions. A.P.R. acknowledges helpful conversations with Nicolás Morales-Durán, Sankar Das Sarma, and Kirill Shtengel. This work was supported by the Air Force Office of Scientific Research (AFOSR) under Award No. FA9550-22-1-0432. The authors acknowledge the MIT SuperCloud and Lincoln Laboratory Supercomputing Center for providing computing resources that have contributed to the research results reported within this paper. N.P. acknowledges a KITP graduate fellowship. A.A was supported by the Knut and Alice Wallenberg Foundation (KAW 2022.0348). L.F. was partly supported by the Simons Investigator Award from the Simons Foundation.

* These authors contributed equally to this work.

- [1] J. Cai, E. Anderson, C. Wang, X. Zhang, X. Liu, W. Holtzmann, Y. Zhang, F. Fan, T. Taniguchi, K. Watanabe, *et al.*, Signatures of fractional quantum anomalous hall states in twisted mote2, *Nature* **1** (2023).
- [2] H. Park, J. Cai, E. Anderson, Y. Zhang, J. Zhu, X. Liu, C. Wang, W. Holtzmann, C. Hu, Z. Liu, *et al.*, Observation of fractionally quantized anomalous hall effect, *Nature* **1** (2023).
- [3] Y. Zeng, Z. Xia, K. Kang, J. Zhu, P. Knüppel, C. Vaswani, K. Watanabe, T. Taniguchi, K. F. Mak, and J. Shan, Thermodynamic evidence of fractional chern insulator in moiré mote2, *Nature* **1** (2023).
- [4] F. Xu, Z. Sun, T. Jia, C. Liu, C. Xu, C. Li, Y. Gu, K. Watanabe, T. Taniguchi, B. Tong, *et al.*, Observation of integer and fractional quantum anomalous hall states in twisted bilayer mote2, arXiv preprint arXiv:2308.06177 (2023).
- [5] Z. Lu, T. Han, Y. Yao, A. P. Reddy, J. Yang, J. Seo, K. Watanabe, T. Taniguchi, L. Fu, and L. Ju, Fractional quantum anomalous Hall effect in multilayer graphene, *Nature* **626**, 759 (2024).
- [6] T. Devakul, V. Crépel, Y. Zhang, and L. Fu, Magic in twisted transition metal dichalcogenide bilayers, *Nature communications* **12**, 6730 (2021).
- [7] H. Li, U. Kumar, K. Sun, and S.-Z. Lin, Spontaneous fractional chern insulators in transition metal dichalcogenide moiré superlattices, *Physical Review Research* **3**, L032070 (2021).
- [8] V. Crépel and L. Fu, Anomalous hall metal and fractional chern insulator in twisted transition metal dichalcogenides, *Physical Review B* **107**, L201109 (2023).
- [9] F. Wu, T. Lovorn, E. Tutuc, I. Martin, and A. MacDonald, Topological insulators in twisted transition metal dichalcogenide homobilayers, *Physical review letters* **122**, 086402 (2019).
- [10] A. Abouelkomans, Z. Liu, and E. J. Bergholtz, Particle-Hole Duality, Emergent Fermi Liquids, and Fractional Chern Insulators in Moiré Flatbands, *Phys. Rev. Lett.* **124**, 106803 (2020).
- [11] P. J. Ledwith, G. Tarnopolsky, E. Khalaf, and A. Vishwanath, Fractional Chern insulator states in twisted bilayer graphene: An analytical approach, *Phys. Rev. Res.* **2**, 023237 (2020).
- [12] C. Repellin and T. Senthil, Chern bands of twisted bilayer graphene: Fractional Chern insulators and spin phase transition, *Phys. Rev. Res.* **2**, 023238 (2020).
- [13] Y. Xie, A. T. Pierce, J. M. Park, D. E. Parker, E. Khalaf, P. Ledwith, Y. Cao, S. H. Lee, S. Chen, P. R. Forrester, *et al.*, Fractional chern insulators in magic-angle twisted bilayer graphene, *Nature* **600**, 439 (2021).
- [14] Q. Gao, J. Dong, P. Ledwith, D. Parker, and E. Khalaf, Untwisting moiré physics: Almost ideal bands and fractional chern insulators in periodically strained monolayer graphene, *Physical Review Letters* **131**, 096401 (2023).
- [15] J. W. Venderbos and L. Fu, Interacting dirac fermions under a spatially alternating pseudomagnetic field: Realization of spontaneous quantum hall effect, *Physical Review B* **93**, 195126 (2016).
- [16] S. A. A. Ghorashi, A. Dunbrack, A. Abouelkomans, J. Sun, X. Du, and J. Cano, Topological and stacked flat

bands in bilayer graphene with a superlattice potential, *Physical Review Letters* **130**, 196201 (2023).

[17] T. Tan, A. P. Reddy, L. Fu, and T. Devakul, Designing topology and fractionalization in narrow gap semiconductor films via electrostatic engineering, arXiv preprint arXiv:2402.03085 (2024).

[18] D. Sheng, Z.-C. Gu, K. Sun, and L. Sheng, Fractional quantum hall effect in the absence of landau levels, *Nature communications* **2**, 389 (2011).

[19] T. Neupert, L. Santos, C. Chamon, and C. Mudry, Fractional quantum hall states at zero magnetic field, *Physical review letters* **106**, 236804 (2011).

[20] N. Regnault and B. A. Bernevig, Fractional chern insulator, *Physical Review X* **1**, 021014 (2011).

[21] E. Tang, J.-W. Mei, and X.-G. Wen, High-temperature fractional quantum hall states, *Physical review letters* **106**, 236802 (2011).

[22] K. Sun, Z. Gu, H. Katsura, and S. D. Sarma, Nearly flatbands with nontrivial topology, *Physical review letters* **106**, 236803 (2011).

[23] R. Willett, J. P. Eisenstein, H. L. Störmer, D. C. Tsui, A. C. Gossard, and J. H. English, Observation of an even-denominator quantum number in the fractional quantum Hall effect, *Phys. Rev. Lett.* **59**, 1776 (1987).

[24] G. Moore and N. Read, Nonabelions in the fractional quantum hall effect, *Nucl. Phys. B* **360**, 362 (1991).

[25] N. Read and D. Green, Paired states of fermions in two dimensions with breaking of parity and time-reversal symmetries and the fractional quantum Hall effect, *Phys. Rev. B* **61**, 10267 (2000).

[26] M. Levin, B. I. Halperin, and B. Rosenow, Particle-Hole Symmetry and the Pfaffian State, *Phys. Rev. Lett.* **99**, 236806 (2007).

[27] N. Read and E. Rezayi, Beyond paired quantum Hall states: Parafermions and incompressible states in the first excited Landau level, *Phys. Rev. B* **59**, 8084 (1999).

[28] E. Witten, Quantum field theory and the Jones polynomial, *Commun. Math. Phys.* **121**, 351 (1989).

[29] K. Fredenhagen, K. H. Rehren, and B. Schroer, Superselection sectors with braid group statistics and exchange algebras, *Commun. Math. Phys.* **125**, 201 (1989).

[30] J. Fröhlich and F. Gabbiani, BRAID STATISTICS IN LOCAL QUANTUM THEORY, *Rev. Math. Phys.* **02**, 251 (1990).

[31] T. D. Imbo, C. Shah Imbo, and E. C. G. Sudarshan, Identical particles, exotic statistics and braid groups, *Phys. Lett. B* **234**, 103 (1990).

[32] A. Yu. Kitaev, Fault-tolerant quantum computation by anyons, *Ann. Phys.* **303**, 2 (2003).

[33] M. Freedman, A. Kitaev, M. Larsen, and Z. Wang, Topological quantum computation, *Bull. Amer. Math. Soc.* **40**, 31 (2003).

[34] C. Nayak, S. H. Simon, A. Stern, M. Freedman, and S. Das Sarma, Non-Abelian anyons and topological quantum computation, *Rev. Mod. Phys.* **80**, 1083 (2008).

[35] B. A. Bernevig and N. Regnault, Emergent many-body translational symmetries of abelian and non-abelian fractionally filled topological insulators, *Physical Review B* **85**, 075128 (2012).

[36] Z. Liu, E. J. Bergholtz, and E. Kapit, Non-Abelian fractional Chern insulators from long-range interactions, *Physical Review B* **88**, 205101 (2013).

[37] D. Wang, Z. Liu, W.-M. Liu, J. Cao, and H. Fan, Fermionic non-abelian fractional chern insulators from dipolar interactions, *Physical Review B* **91**, 125138 (2015).

[38] A. Kitaev, Anyons in an exactly solved model and beyond, *Ann. Phys.* **321**, 2 (2006).

[39] G. Jackeli and G. Khaliullin, Mott Insulators in the Strong Spin-Orbit Coupling Limit: From Heisenberg to a Quantum Compass and Kitaev Models, *Phys. Rev. Lett.* **102**, 017205 (2009).

[40] A. P. Reddy, F. Alsallom, Y. Zhang, T. Devakul, and L. Fu, Fractional quantum anomalous hall states in twisted bilayer mote₂ and wse₂, *Phys. Rev. B* **108**, 085117 (2023).

[41] N. Morales-Durán, N. Wei, J. Shi, and A. H. MacDonald, Magic angles and fractional chern insulators in twisted homobilayer transition metal dichalcogenides, *Phys. Rev. Lett.* **132**, 096602 (2024).

[42] P. Bruno, V. Dugaev, and M. Taillefumier, Topological hall effect and berry phase in magnetic nanostructures, *Physical review letters* **93**, 096806 (2004).

[43] J. H. Han, *Skyrmions in Condensed Matter* (Springer International Publishing, Cham, Switzerland, 2017).

[44] K. Hamamoto, M. Ezawa, and N. Nagaosa, Quantized topological Hall effect in skyrmion crystal, *Phys. Rev. B* **92**, 115417 (2015).

[45] N. Paul, Y. Zhang, and L. Fu, Giant proximity exchange and flat chern band in 2d magnet-semiconductor heterostructures, *Science Advances* **9**, eabn1401 (2023).

[46] M. Akram, H. LaBollita, D. Dey, J. Kapeghian, O. Erten, and A. S. Botana, Moiré Skyrmions and Chiral Magnetic Phases in Twisted CrX₃ (X = I, Br, and Cl) Bilayers, *Nano Lett.* 10.1021/acs.nanolett.1c02096 (2021).

[47] K. Hejazi, Z.-X. Luo, and L. Balents, Noncollinear phases in moiré magnets, *Proc. Natl. Acad. Sci. U.S.A.* **117**, 10721 (2020).

[48] K. Hejazi, Z.-X. Luo, and L. Balents, Heterobilayer moiré magnets: Moiré skyrmions and commensurate-incommensurate transitions, *Phys. Rev. B* **104**, L100406 (2021).

[49] P. Bruno, V. K. Dugaev, and M. Taillefumier, Topological Hall Effect and Berry Phase in Magnetic Nanostructures, *Phys. Rev. Lett.* **93**, 096806 (2004).

[50] E. Anderson, F.-R. Fan, J. Cai, W. Holtzmann, T. Taniguchi, K. Watanabe, D. Xiao, W. Yao, and X. Xu, Programming correlated magnetic states with gate-controlled moiré geometry, *Science* **381**, 325 (2023).

[51] N. Morales-Durán, J. Wang, G. R. Schleder, M. Angeli, Z. Zhu, E. Kaxiras, C. Repellin, and J. Cano, Pressure-enhanced fractional chern insulators along a magic line in moiré transition metal dichalcogenides, *Physical Review Research* **5**, L032022 (2023).

[52] C. Wang, X.-W. Zhang, X. Liu, Y. He, X. Xu, Y. Ran, T. Cao, and D. Xiao, Fractional Chern Insulator in Twisted Bilayer MoTe₂, arXiv 10.48550/arXiv.2304.11864 (2023), 2304.11864.

[53] A. P. Reddy and L. Fu, Toward a global phase diagram of the fractional quantum anomalous hall effect, arXiv preprint arXiv:2308.10406 (2023).

[54] K. Karube, J. S. White, D. Morikawa, M. Bartkowiak, A. Kikkawa, Y. Tokunaga, T. Arima, H. M. Rønnow, Y. Tokura, and Y. Taguchi, Skyrmion formation in a bulk chiral magnet at zero magnetic field and above room temperature, *Phys. Rev. Mater.* **1**, 074405 (2017).

[55] J.-H. Park and J. H. Han, Zero-temperature phases for chiral magnets in three dimensions, *Phys. Rev. B* **83**,

184406 (2011).

[56] Y. Tokura and N. Kanazawa, Magnetic Skyrmion Materials, *Chem. Rev.* 10.1021/acs.chemrev.0c00297 (2020).

[57] S.-Z. Lin and S. Hayami, Ginzburg-landau theory for skyrmions in inversion-symmetric magnets with competing interactions, *Phys. Rev. B* **93**, 064430 (2016).

[58] A. Tonomura, X. Yu, K. Yanagisawa, T. Matsuda, Y. Onose, N. Kanazawa, H. S. Park, and Y. Tokura, Real-space observation of skyrmion lattice in helimagnet mnsi thin samples, *Nano Lett.* **12**, 1673 (2012).

[59] M. Oshikawa, Y. B. Kim, K. Shtengel, C. Nayak, and S. Tewari, Topological degeneracy of non-Abelian states for dummies, *Ann. Phys.* **322**, 1477 (2007).

[60] M. R. Peterson, T. Jolicoeur, and S. D. Sarma, Finite-layer thickness stabilizes the pfaffian state for the 5/2 fractional quantum hall effect: wave function overlap and topological degeneracy, *Physical review letters* **101**, 016807 (2008).

[61] H. Wang, D. Sheng, and F. Haldane, Particle-hole symmetry breaking and the $\nu = 5/2$ fractional quantum hall effect, *Physical Review B* **80**, 241311 (2009).

[62] K. Pakrouski, M. R. Peterson, T. Jolicoeur, V. W. Scarola, C. Nayak, and M. Troyer, Phase diagram of the $\nu = 5/2$ fractional quantum hall effect: effects of landau-level mixing and nonzero width, *Physical Review X* **5**, 021004 (2015).

[63] M. Banerjee, M. Heiblum, V. Umansky, D. E. Feldman, Y. Oreg, and A. Stern, Observation of half-integer thermal hall conductance, *Nature* **559**, 205 (2018).

[64] M. Greiter, X.-G. Wen, and F. Wilczek, Paired hall state at half filling, *Physical review letters* **66**, 3205 (1991).

[65] M. Greiter, X.-G. Wen, and F. Wilczek, Paired hall states, *Nuclear Physics B* **374**, 567 (1992).

[66] E. H. Rezayi and F. D. M. Haldane, Incompressible paired hall state, stripe order, and the composite fermion liquid phase in half-filled landau levels, *Physical Review Letters* **84**, 4685 (2000).

[67] S.-S. Lee, S. Ryu, C. Nayak, and M. P. Fisher, Particle-hole symmetry and the $\nu = 5/2$ quantum hall state, *Physical review letters* **99**, 236807 (2007).

[68] M. Levin, B. I. Halperin, and B. Rosenow, Particle-hole symmetry and the pfaffian state, *Physical review letters* **99**, 236806 (2007).

[69] Y. Onishi and L. Fu, Quantum weight, *arXiv preprint arXiv:2401.13847* (2024).

[70] Y. Onishi and L. Fu, Quantum geometry, optical absorption and topological gap bound, *arXiv preprint arXiv:2306.00078* (2023).

[71] T. Ozawa and B. Mera, Relations between topology and the quantum metric for chern insulators, *Physical Review B* **104**, 045103 (2021).

[72] K. Kang, B. Shen, Y. Qiu, K. Watanabe, T. Taniguchi, J. Shan, and K. F. Mak, Observation of the fractional quantum spin hall effect in moiré mote2, *arXiv preprint arXiv:2402.03294* (2024).

[73] K. Kang, Y. Qiu, K. Watanabe, T. Taniguchi, J. Shan, and K. F. Mak, Observation of the double quantum spin hall phase in moiré wse2, *arXiv preprint arXiv:2402.04196* (2024).

[74] Q. Shi, E.-M. Shih, M. V. Gustafsson, D. A. Rhodes, B. Kim, K. Watanabe, T. Taniguchi, Z. Papić, J. Hone, and C. R. Dean, Odd-and even-denominator fractional quantum hall states in monolayer wse2, *Nature Nanotechnology* **15**, 569 (2020).

[75] J. Pack, Y. Guo, Z. Liu, B. S. Jessen, L. Holtzman, S. Liu, M. Cothrine, K. Watanabe, T. Taniguchi, D. G. Mandrus, *et al.*, Charge-transfer contact to a high-mobility monolayer semiconductor, *arXiv preprint arXiv:2310.19782* (2023).